Journal of Applied Polymer Science

Directional self-assembly by electrospun wet fibers

Xiaoming Guo,[1] Yongyi Yao,[1] Tao Zhou,[1,2] Ruili Xiang,[3] Minzhu Chen[4]
[1]Textile Institute, Sichuan University, Chengdu 610065, Sichuan, People's Republic of China
[2]Chengdu Biotop Pharma Technology Company, Limited, Chengdu 610065, Sichuan, People's Republic of China
[3]Analytical and Testing Centre, Sichuan University, Chengdu 610064, Sichuan, People's Republic of China
[4]College of Chemistry, Sichuan University, Chengdu 610064, Sichuan, People's Republic of China
Correspondence to: Y. Yao (E-mail: yongyiyao@scu.edu.cn)

ABSTRACT: In this study, we examined directional self-assembly by electrospun wet fibers. The landing point of the wet fibers was controllable as its trajectory was strictly limited by the adjustment of the parameters of electrospinning. The wet fibers would not stack on the grounded plate in an irregular pattern but in the direction of an electric field in sequence. The preliminary wet fibers deposited and erected on the ground plate to form a controllable circle. The subsequent wet fibers traveled to the top of the circle directionally to organize a mesh tube. The apical circle of the mesh tube was the precise landing point of the subsequent wet fibers. With the wet fibers landing continuously, the mesh tube grew longer and longer. Finally, the controllable circle grew to be the growing mesh tube step by step. We discovered that the mesh tube was assembled by fibers spontaneously in the electrostatic field. In this article, we also try to explain the mechanism of self-assembly and the formation of wet fibers. © 2015 Wiley Periodicals, Inc. J. Appl. Polym. Sci. **2016**, *133*, 43003.

KEYWORDS: electrospinning; fibers; self-assembly

Received 10 July 2015; accepted 1 October 2015
DOI: 10.1002/app.43003

INTRODUCTION

Self-assembly, whose basic structure unit is usually a molecule, macromolecule, or nanoscale building blocks, has been extensively researched for many years.[1–12] The novel superstructures of the self-assembled aggregation provided excellent performance for the aggregation. Therefore, the technique has tremendous application prospects for drug release, electrochemistry, bioengineering, catalysis, tissue engineering, and more. There are several forces (e.g., van der Waals, electrostatic, magnetic, molecular, and entropic forces) that can drive the achievement of self-assembly. Each basic structure unit is assembled into the aggregation by a different force. The electrostatic self-assembly technology, which uses an electrostatic force to achieve the process of self-assembly, has gotten more attention in past years.[13–18] As one of the electrostatic self-assembly technologies, researchers have focused on electrospinning as well.

In electrospinning, a high electrostatic voltage is applied between the capillary tube that contains the spinning solution and the grounded electrode to create an electrically charged jet.[19] As the intensity of the electric field increased, the fluid at the tip of the capillary tube elongated to form a Taylor cone.[20] Then, the electric field drives the liquid electrostatic force to overcome the surface tension, and the charged jet of the fluid is ejected from the tip of the Taylor cone.[21] Undergoing an instability and elongation process, accompanied by whipping, splitting, and solvent evaporation,[22–26] the fibers were solidified and deposited on the grounded collector, and those fibers formed a flat nonwoven mat. Although some researchers have assembled the fibers to form various patterns,[27–32] the precise directional self-assembly to a fibrous aggregation form with a regular shape is rarely realized. In those previous reports, fibers stacked on the grounded prepatterned conductive collector or template in an irregular state still. However, it is just right that the fibers stacked in an irregular state hindered directional self-assembly. To realize the directional self-assembly, an effective method is to control the trajectory of the fibers.

In this study, we determined that the directional self-assembly could be achieved by the electrospinning of wet fibers. We also determined the best combination of parameters to assemble a mesh tube (see Supporting Information). The trajectory of the wet fibers was strictly limited by the adjustment of the parameters of electrospinning after the mesh tube was assembled. The fibers would not stack on the grounded plate in an irregular

Additional Supporting Information may be found in the online version of this article.

state any more but in the direction of the electric field in a sequence. The preliminary fibers deposited and erected on the ground plate to form a controllable circle. The subsequent fibers directionally traveled to the top of the circle to form a mesh tube. The apical circle of the mesh tube was the precise landing point of the subsequent fibers. Finally, the controllable circle grew step by step to be a growing mesh tube.

EXPERIMENTAL

Synthesis of Polyacrylonitrile (PAN)

Acrylonitrile (Shandong Xiya) was initiated by azobisisobutyronitrile (AIBN; Chengdu Cdkelong at 60°C for 6 h in the solvent of dimethyl sulfoxide (DMSO; Chengdu Cdkelong) to prepare PAN (weight-average molecular weight = 189,000, weight-average molecular weight/number-average molecular weight = 2.805). Then, PAN was precipitated in the water phase for 24 h and dried at 60°C in a vacuum oven for 12 h. Finally, PAN was dissolved in DMSO at a concentration of 13 wt % for electrospinning.

Preparation of the Electrospinning Dope

The PAN/DMSO solution was loaded into a syringe, which was connected to a ZGF negative high-voltage DC power supply (Chengdu Chuandianhuayun) and an LSP01-1A injection pump (Baoding Longerpump). The applied spinning voltage in this study was −17 kV, the vertical distance from the needle to the collector was 20 cm, and the feed rate of the pump was 150 μm/min. A large grounded electrode (30 × 30 cm^2) wrapped in aluminum foil and an insulating base with a grounded rod (diameter equals to 3 mm) in the center of it were applied in this experiment. The room temperature was 15–20°C, and the ambient humidity was from 40 to 80% relative humidity.

Characterization

Scanning electron microscopy (SEM) images were obtained to investigate the morphology of the sample surface with a JEOL JSM-7500F SEM. The SEM images were analyzed with the Image-Pro Plus image analysis program. Optical microscopy photos were obtained with a JNOEC DN-10B optical microscope.

RESULTS AND DISCUSSION

In typical experiment, we chose PAN/DMSO as a solution system, so the wet fibers could be fabricated by electrospun PAN/DMSO. To contrast with the wet fibers, dry fibers were also fabricated with electrospun PAN/dimethylformamide (DMF). The solvent used in the polymer solutions was significant because an appropriate solvent system is indispensable for successful electrospinning and the production of ultrafine nanofibers.[33] To focus on the morphology, structure, and size of fibers, DMSO is not the primary choice, unlike DMF for electrospun PAN, and is always being ignored. However, the high boiling point, large surface tension, and strong intermolecular interactions between the PAN macromolecules and DMSO molecules caused the fibers fabricated by electrospinning to be in a liquid state.[27]

Formation of the Thin-Walled Mesh Tube

On the basis of the formation of the wet fibers, a controllable fibrous mesh tube, shown in Figure 1(a,b), was self-assembled by the control of the parameters of electrospinning the dope of PAN/DMSO. The self-assembly occurred rapidly, directionally, continuously, and steadily (Movies S1 and S2, Supporting Information) The size of the fibrous mesh tube could be controlled through the adjustment of the voltage and the size of the grounded electrode. To explain the formation of the fibrous mesh tube received by the grounded plate electrode, a schematic diagram is shown in Figure 1(d), which includes two stages: the transitional stage and the stable stage.

The transition stage occurred first. Preliminary fibers landed upright in the grounded plate electrode, where they formed a controllable circle, which was erected and fixed. With respect to sustainability, all of the ejected fibers subsequently travelled to the apical circle of the mesh tube, which consisted of the fixed fibers directionally, orderly, and continuously stacked. The mesh tube grew in the direction from the grounded plate to the needle as the fibers stacked constantly. This was totally different with the conventional electrospinning, obviously, where the fibers just deposited on the received device in an irregular way to form a flat nonwoven mat, as shown in Figure 1(c), and the fibers always filled the entire receiving area and could not form a circle with a few fibers in the inner region or erect simultaneously. In the transition stage, the height of the mesh tube increased, and the diameter of the mesh tube (D_a) decreased. D_a shrank to a minimum value because of the effect of the electric field. After D_a reached a stable value, the transition stage transformed to the stable stage. The mesh tube grew toward to the needle as more and more fibers were overlapped and erected in the apical circle of the mesh tube. The top of the mesh tube experienced electrostatic attraction from the needle. At the same time, the electrostatic attraction also led to a decrease in the diameter as the stronger attraction from the electric field was strengthened between the needle and the apical circle of the mesh tube. When the amount of overlapped fibers increased, the gravity of the mesh tube gradually increased. When gravity was equal to the electrostatic attraction, the mesh tube did not increase any more. When more fibers landed in the top of the mesh tube, the mesh tube did not keep the balance of gravity and electrostatic attraction. The distance between the top of the mesh tube and the needle (D_s) remained stable. The fibrous mesh tube grew constantly step by step.

When a grounded rod electrode was used for the received fibers instead of the grounded plate electrode, the preliminary fibers were fixed on the top point of the ground rod. In the transition stage, D_a increased to a stable value from zero. When the mesh tube was just fixed on the top point of the grounded rod, where it was fixed onto the plate to form a circle, it was easily driven by external forces. So the mesh tube rotated counterclockwise around the grounded rod as the fibers whipped counterclockwise; this provided provide kinetic energy for mesh tube. Also, the mesh tube gradually twisted into fiber bundles. In the stable stage, the value of D_a and D_s was greatly influenced by the voltage. D_a and D_s decreased with gradually increasing voltage. As shown in Table I, with increasing voltage from −17 to −21 kV, D_a and D_s decreased from 3.3 and 3, respectively, to 0 cm.

Mechanism of the Self-Assembly Process by Electrospinning

As mentioned previously, the mesh tube was assembled by wet fibers, so it is necessary to discuss the mechanism of self-

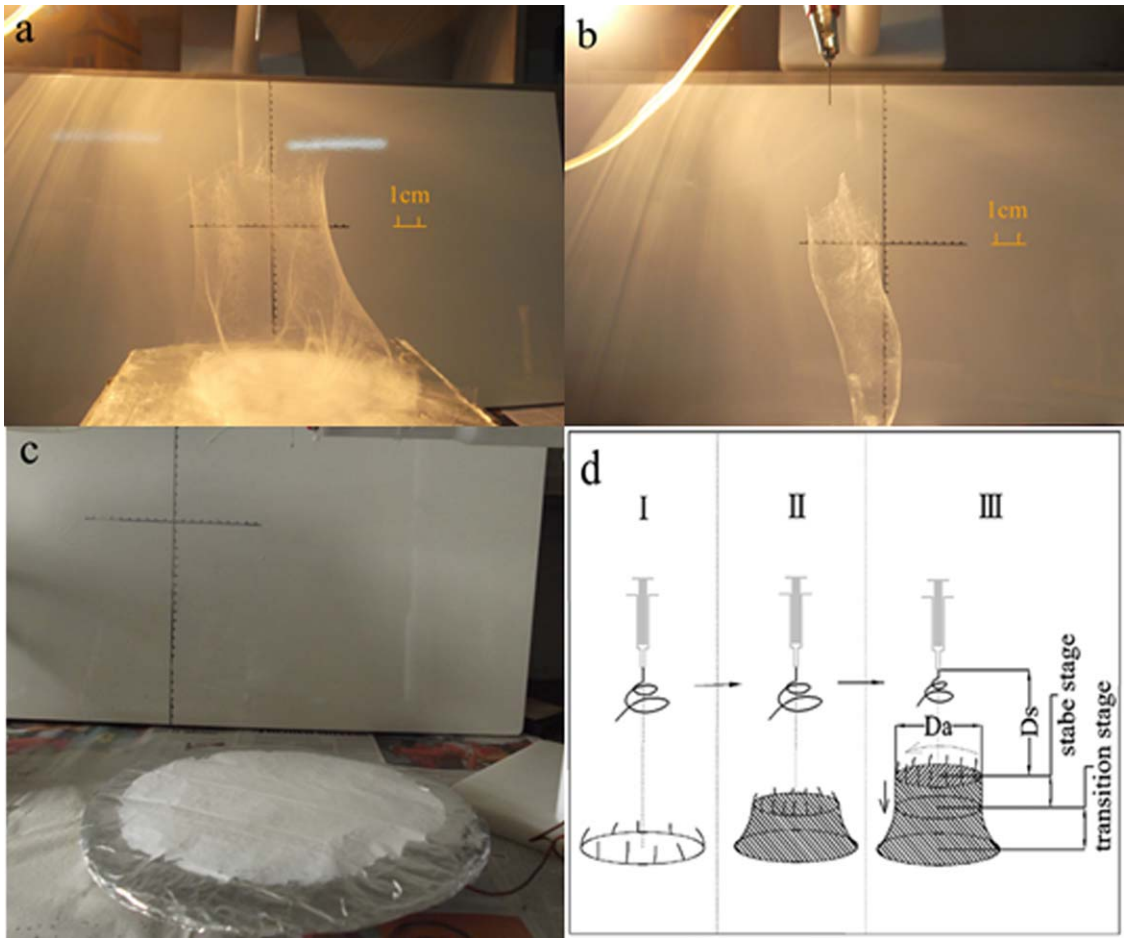

Figure 1. (a) Mesh tube received by a grounded plate electrode. (b) Mesh tube received by a grounded rod electrode. (c) Flat nonwoven mat consisting of dry fibers received by a grounded plate electrode. (d) Schematic diagram of the formation of the mesh tube. [Color figure can be viewed in the online issue, which is available at wileyonlinelibrary.com.]

assembly by wet fibers via electrospinning. When the preliminary fibers fell onto the grounded plate, they erected in the electric field when their bottom was fixed. A similar phenomenon was reported by Frenot *et al.*[34] We supposed that the fibers had a positive charge that corresponded to the inverse of the field in which they were situated. The fibers were affected as if they were in a field with a zero potential. The salt played an important role in that system, as the existence of anions and cations made the fibers conductive, and the solvent LiCl/Dimethylacetamide (DMAc) was not volatile. This provided a channel for ion transport. DMSO and LiCl/DMAc were similar in that they both had a high boiling point and they were both electroconductive. Although there were no anions and cations in the PAN/DMSO solution, we concluded that the fibers were electroconductive as a large number of solvents persisted in the wet fibers. As the mesh tube grew toward to the needle, the electric field intensity between the needle and the top of the mesh tube increased with declining distance. So, the shortening of the distance between them did not hinder the formation of fibers. Also, the enhanced electric field made the reborn fibers land on the top of the mesh tube directionally and continually; this made the self-assembly behavior realizable. What we need to emphasize is that all of fibers flew to the top of the preliminary fibers, and no fibers deposited anywhere else (Movie S3, Supporting Information); this has not been realized over past decades. Contrary to traditional electrospinning, whose fibers are collected in an irregular to form on a flat nonwoven mat, we observed that the trajectory of the wet fibers was strictly limited by the adjustment of the parameters of electrospinning, as shown in Figure 2. The erect wet fibers provided an enhanced electric field, which drove the fibers to be ejected subsequently, just travelling to the apical circle of the mesh tube directionally and orderly.

Table I. Changes in D_a and D_s with Increasing Voltage

Voltage (kV)	−17.0	−18.0	−19.0	−20.0	−21.0
D_a (cm)	3.3	2.9	2.1	1.5	0
D_s (cm)	3.0	2.8	2.0	1.0	0

Wet Fibers

Actually, the wet fibers [shown in Figure 3(b)] were observed with an optical microscope to contrast them with the dry fibers [shown in Figure 3(a)]. We electrospun the same concentrations of solutions of PAN/DMSO and PAN/DMF into nanofibers with the same experimental parameters (details in the Supporting

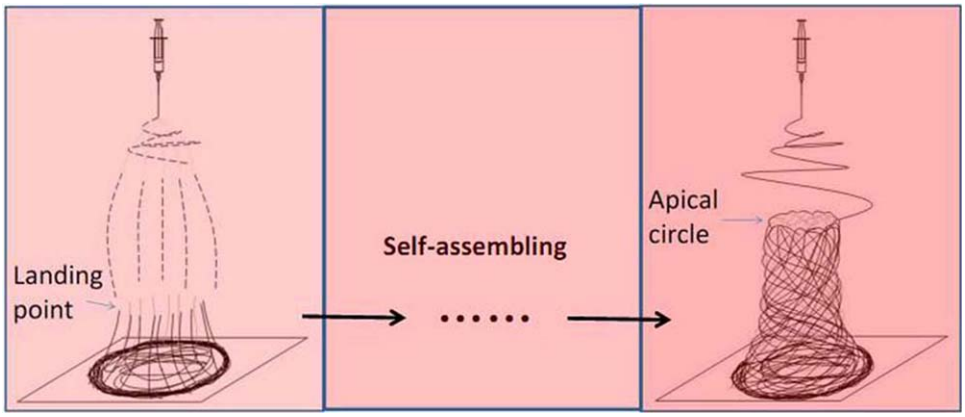

Figure 2. Simulated diagram of the self-assembly of wet fibers. [Color figure can be viewed in the online issue, which is available at wileyonlinelibrary.com.]

Information) to contrast the morphologies of the two kinds of fibers. There were a few residual solvents observed in the fibers fabricated by the electrospun PAN/DMF. However, the fibers originating from the electrospun PAN/DMSO were full of solvents. To quantify the residues of solvents on the two kinds of fibers, we calculated the mass fraction of residual solvents in the fibers. As shown in Table II, the content of solvents in the fibers was quite different when different solvents were used. Dry fibers and wet fibers were received by a grounded roller wrapped in aluminum foil. The residues of the solvents in the fibers were lower than 5 wt % in the PAN/DMF spinning solution, whereas the residues of solvents in the wet fibers were higher than 80 wt % in the PAN/DMSO spinning solution. We inferred that the fibers were selected in the gel state. In a comparison of the residues of solvent in the fibers film selected by rollers with the mesh tube, it was apparent that a fraction of the solvent was volatile. However, to observe the amounts of solvents in the mesh tube and the initial solution, it was quite inconceivable that their solvent contents were equal. That means that there was basically no loss of solvent in the process of the electrospinning of PAN/DMSO into fibers. This further confirmed that the strong intermolecular interactions, high boiling point, and large surface tension lead to the formation of stabilized wet fibers.

The formation of the wet fibers was probably due to the physical gelation of fibers. A physical gel could form in the PAN solution after the aging process via the physical crosslinking of PAN molecules because the presence of a permanent dipole in the monomer unit caused by the bulky nitrile group with strong polarity interact with proper solvent(DMSO) made it possible.[35] The solution properties were an important factor of gelation behavior in PAN/DMSO. The intermolecular interactions had a more decisive effect on the physical properties of the PAN/DMSO solutions. The strong polar nitrile group of PAN could polarize the solvent molecules; this made the polarized DMSO molecules orient to form lots of solvent bridges between the nitrile groups.[36] Corresponding to the polarizing effect, DMSO molecules, which had a more consistent polarization, made the PAN solutions more stable and able to tolerate environmental conditions. So, when the environmental conditions changed fast enough, the evaporation of DMSO was greatly hampered, and the gelation of fibers was achieved quickly by electrospinning in the formation of wet fibers.

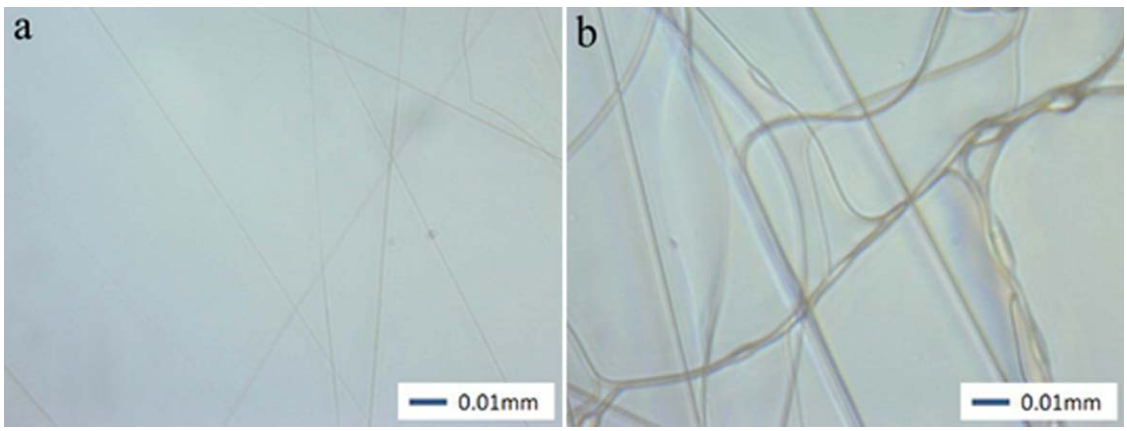

Figure 3. Optical microscopy photograph: (a) dry fibers fabricated from the electrospun dope of PAN/DMF and (b) wet fibers fabricated from the electrospun dope of PAN/DMSO. [Color figure can be viewed in the online issue, which is available at wileyonlinelibrary.com.]

Table II. Mass Fractions of the Residual Solvents in the Dry Fibers, Wet Fibers, and Mesh Tube

Concentration of the dope (%)	10	11.5	13	13.5	15
Dry fibers (%)	4.9	4.8	4.4	3.2	1.9
Wet fibers (%)	88.6	87.5	86.7	83.8	82.1
Mesh tube (%)	89.0	88.5	87.0	85.5	84.0

Morphologies of the Fibers

The determined mean diameter of the fibers in the mesh tube was 609 ± 250 nm [Figure 4(b,d)], but it was only 304 ± 130 nm [Figure 4(a,c)] for the electrospun PAN/DMF. This was because the larger surface tension of PAN/DMSO led to the generation of thicker fibers. Although D_s was only several centimeters, which was less than the receiving distance of conventional electrospinning, the fibers still fabricated on the nanoscale; this indicated that the process of the formation of fibers was achieved.

By observing the SEM of fibers in the mesh tube, we observed that there was a fusion phenomenon [Figure 4(b)] occurring in the overlapping of the fibers. We inferred that the solvents had relative mobility in the wet fibers that were in the liquid state. So, the solvents could move from one fiber to the other through overlap when the two fibers were stacked. As the solvents could not be removed easily under mild environmental conditions, the stacked fibers fused gradually at the overlap. This was very significant for the fabrication of crosslinked fiber membranes.

CONCLUSIONS

We observed that directional self-assembly could be realized by electrospun wet fibers when the trajectory of the wet fibers was strictly limited by adjustment of the parameters of electrospinning. The wet fibers persisted in lots of solvents in the liquid state; this made them conductive. The conductivity of the wet fibers made them erect and orient in the direction of the electric field; this led a decrease in the distance between the needle and the top of the erect fibers and a corresponding increase in the electric field increases. The enhanced electric field limited the trajectory of the wet fibers and drove them to just travel to the top of the previously erected fibers. The self-assembly of the mesh tube was achieved step by step as the wet fibers stacked in the direction of the electric field to organize the wall of the mesh tube. Meanwhile, we also found by observing the morphology of the fibers of the tube wall that there was a fusion phenomenon occurring in the overlap of fibers. We considered that it was very significant for the fabrication of the crosslinked fiber membranes.

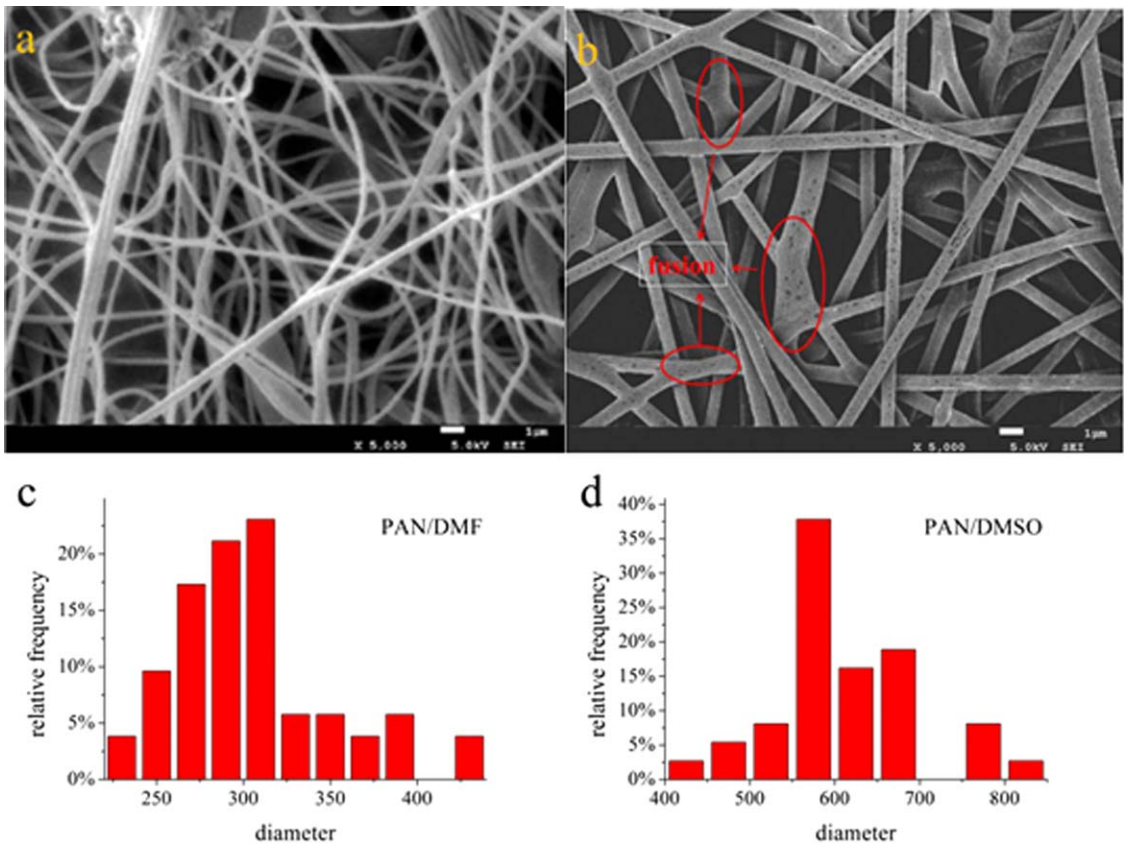

Figure 4. SEM micrograph and diameter distributions of the fibers: (a) dry fibers fabricated from the electrospun dope of PAN/DMF, (b) wet fibers in the mesh tube fabricated from the electrospun dope of PAN/DMSO, (c) diameter distributions of dry fibers, and (d) diameter distributions of wet fibers in the mesh tube. [Color figure can be viewed in the online issue, which is available at wileyonlinelibrary.com.]

ACKNOWLEDGMENTS

This work was supported by the National Natural Science Foundation of the People's Republic of China (contract grant number 50473050) and by the Application and Basic Research Foundation of Sichuan Province (contract grant number 2010JY0015).

REFERENCES

1. Claudia, P.; Andreas, K.; Horst, W. *Angew. Chem. Int. Ed.* **2001**, *41*, 1188.
2. Colfen, H.; Mann, S. *Angew. Chem. Int. Ed. Engl.* **2003**, *42*, 2350.
3. Daniel, L.; Kai, S. *Science* **2010**, *327*, 46.
4. George, M. W.; Bartosz, G. *Science* **2002**, *295*, 2418.
5. Marek, G.; Jan, V.; Eric, M. F.; Luis, M. L.-M. *ACS Nano* **2010**, *4*, 3591.
6. Meital, R.; Ehud, G. *Science* **2003**, *300*, 625.
7. Michael, E.; Joshua, P. S.; Mathias, S.; Marcus, F.; Alexander, A. G.; Mark, C. H.; Phaedon, A. *ACS Nano* **2008**, *2*, 2445.
8. Rothemund, P. W. *Nature* **2006**, *440*, 297.
9. Russell, S. S.; Peter, J. S. *ChemInform* **2003**, *34*, 972.
10. Sang, O. K.; Harun, H. S.; Mark, P. S.; Nicola, J. F.; Juan, J. D. P.; Paul, F. N. *Nature* **2003**, *424*, 411.
11. Zhang, S. *Nat. Biotechnol.* **2003**, *21*, 1171.
12. Zhiyong, T.; Kotov, N. A.; Michael, G. *Science* **2002**, *297*, 237.
13. Kalsin, A. M. *Science* **2006**, *312*, 420.
14. Seung-Sub, L.; Ki-Bong, L.; Jong-Dal, H. *Langmuir* **2003**, *19*, 7592.
15. Hanna, P.; Marjo, L.; Timo, A.; Sami, A.; Jarkko, L.; Markku, H.; Keijo, H.; Jukka, L. *Langmuir* **2005**, *22*, 74.
16. Shen, J.; Hu, Y.; Li, C.; Qin, C.; Shi, M.; Ye, M. *Langmuir* **2009**, *25*, 6122.
17. Jianping, G.; Yongxing, H.; Tierui, Z.; Tuan, H.; Yadong, Y. *Langmuir* **2008**, *24*, 3671.
18. Fang, Y.; Guo, S.; Zhu, C.; Zhai, Y.; Wang, E. *Langmuir* **2010**, *26*, 11277.
19. Huang, Z.-M.; Zhang, Y. Z.; Kotaki, M.; Ramakrishna, S. *Compos. Sci. Technol.* **2003**, *63*, 2223.
20. Yarin, A. L.; Koombhongse, S.; Reneker, D. H. *J. Appl. Phys.* **2001**, *90*, 4836.
21. Reneker, D. H.; Yarin, A. L. *Polymer* **2008**, *49*, 2387.
22. Reneker, D. H.; Yarin, A. L.; Fong, H.; Koombhongse, S. *J. Appl. Phys.* **2000**, *87*, 4531.
23. De Vrieze, S.; Van Camp, T.; Nelvig, A.; Hagström, B.; Westbroek, P.; De Clerck, K. *J. Mater. Sci.* **2008**, *44*, 1357.
24. Subbiah, T.; Bhat, G. S.; Tock, R. W.; Parameswaran, S.; Ramkumar, S. S. *J. Appl. Polym. Sci.* **2005**, *96*, 557.
25. Shin, Y. M.; Hohman, M. M.; Brenner, M. P.; Rutledge, G. C. *Appl. Phys. Lett.* **2001**, *78*, 1149.
26. Shin, Y. M.; Hohman, M. M.; Brenner, M. P.; Rutledge, G. C. *Polymer* **2001**, *42*, 09955.
27. Yan, G.; Yu, J.; Qiu, Y.; Yi, X.; Lu, J.; Zhou, X.; Bai, X. *Langmuir* **2011**, *27*, 4285.
28. Meng, F.; Zhan, Y.; Lei, Y.; Zhao, R.; Xu, M.; Liu, X. *Eur. Polym. J.* **2011**, *47*, 1563.
29. Paneva, D.; Manolova, N.; Rashkov, I.; Penchev, H.; Mihal, M.; Dragan, E. S. *Dig. J. Nanomater. Biostruct.* **2010**, *5*, 811.
30. Reis, T. C.; Correia, I. J.; Aguiar-Ricardo, A. *Nanoscale* **2013**, *5*, 7528.
31. Sun, B.; Long, Y. Z.; Zhang, H. D.; Li, M. M.; Duvail, J. L.; Jiang, X. Y.; Yin, H. L. *Prog. Polym. Sci.* **2014**, *39*, 862.
32. Sun, B.; Jiang, X. J.; Zhang, S. C.; Zhang, J. C.; Li, Y. F.; You, Q. Z.; Long, Y. Z. *J. Mater. Chem. B* **2015**, *3*, 5389.
33. Bhardwaj, N.; Kundu, S. C. *Biotechnol. Adv.* **2010**, *28*, 325.
34. Frenot, A.; Henriksson, M. W.; Walkenström, P. *J. Appl. Polym. Sci.* **2007**, *103*, 1473.
35. Tan, L.; Pan, D.; Pan, N. *Polymer* **2008**, *49*, 5676.
36. Eom, Y.; Kim, B. C. *Polymer* **2014**, *55*, 2570.